

Seeking for Simplicity in Complex Networks

Luciano da Fontoura Costa*

Instituto de Física de São Carlos, Universidade de São Paulo, Av. Trabalhador São Carlense 400, Caixa Postal 369, CEP 13560-970, São Carlos, São Paulo, Brazil

(Dated: 27th Jan 2007)

Complex networks can be understood as graphs whose connectivity deviates from those of regular or near-regular graphs (which can be understood as ‘simple’). While a great deal of the attention so far dedicated to complex networks has been duly driven by the above principle, in this work we take the dual approach and address the identification of simplicity, in the sense of regularity, in complex networks. The basic idea is to seek for subgraphs exhibiting small dispersion (e.g. standard deviation or entropy) of local measurements such as the node degree and clustering coefficient. Here we consider two types of subgraphs: (a) those defined by the progressive neighborhoods around each node and (b) subgraphs obtained from sets of nodes presenting similar local measurements. The former approach allows the assignment of a hierarchical regularity index to all network nodes, the latter paves the way for the identification of subgraphs (patches) in the original network, with nearly uniform connectivity. We illustrate the potential of such methods with respect to four classical network models (i.e. Erdős-Rényi, Barabási-Albert, Watts-Strogatz as well as a geographical model) as well as to seven real-world networks (i.e. word associations, cortical networks, protein-protein interaction, football league and flights). Several interesting results and insights are obtained with respect to both theoretical and real-world networks.

‘Simplicity is the ultimate sophistication.’ (Leonardo da Vinci)

I. INTRODUCTION

Although difficult to be defined individually, simplicity and complexity are unquestionably opposite concepts. A great deal of the efforts and advances in science and technology along the recent decades has been intrinsically related to the dichotomy simplicity/complexity (e.g. [1]). For instance, while linear systems are characterized by relatively simple attractors, non-linear chaotic dynamics give rise to highly complex fractal attractors (e.g. [2]). At the same time, the origin of the now ubiquitous complex networks was ultimately motivated by the identification that graphs obtained from natural or human-made structures tended to present intricate connectivity when compared to regular (e.g. lattices and meshes) or nearly-regular graphs (e.g. the Erdős-Rényi model). Given their structured connectivity, complex networks have provided excellent models for a series of ‘complex’ real-world systems ranging from the Internet to protein-protein interaction (e.g. [3, 4, 5, 6, 7]).

Having understood and tamed the simpler, usually linear, systems, science is now bound by the ‘complexities’ pervading the universe. Yet, while it is important to focus the characterization and modeling of such complexities, it is also useful to adopt the opposite approach of seeking for simplicity and regularity in the analyzed systems. After all, having properly defined simplicity, complexity should correspond just to the opposite. One

related example is the identification of the windows of periodicity (‘simplicity’) in chaotic iterated series (e.g. [2]). The purpose of the present work is precisely to develop means to identify simplicity and regularity in complex networks in order not only to obtain better characterization of such structures, but also to reassess such networks in terms of their original motivation, i.e. how much they depart from regular or near-regular graphs. The motivation for finding regularities in complex networks includes but is by no means limited to the following facts: (1) the properties and distribution of regular patches can help the characterization, understanding and modeling of complex networks; (2) the presence of regular patches in a complex network may suggest a hybrid nature of that network (e.g. a combination of the regular and scale-free paradigms); and (3) regular patches can have strong influence on dynamical processes taking place on the network.

In graph theory, a regular graph is characterized by having all its nodes with exactly the same degree. However, such a definition is limited in the sense that it is still possible to obtain a large diversity of such ‘regular’ graphs. Figure 1 presents three examples of ‘regular’ graphs. All nodes in these graphs exhibit the same degree, equal to four. While the infinite structures in (a) and (c) have more ‘regular’ connectivity, the graph in (b) looks rather irregular. Actually, even the structure in (c) has irregularities if we consider measurements such as the individual clustering coefficient. It is clear from such an example that identical node degree is not enough to ensure uniform connectivity.

Because we are interested in characterizing and identifying regularity (i.e. ‘simplicity’) in complex networks, the first important step consists of stating clearly what is meant by regularity, uniformity or simplicity. Perhaps the most strict imposition of regularity on a net-

*Electronic address: luciano@if.sc.usp.br

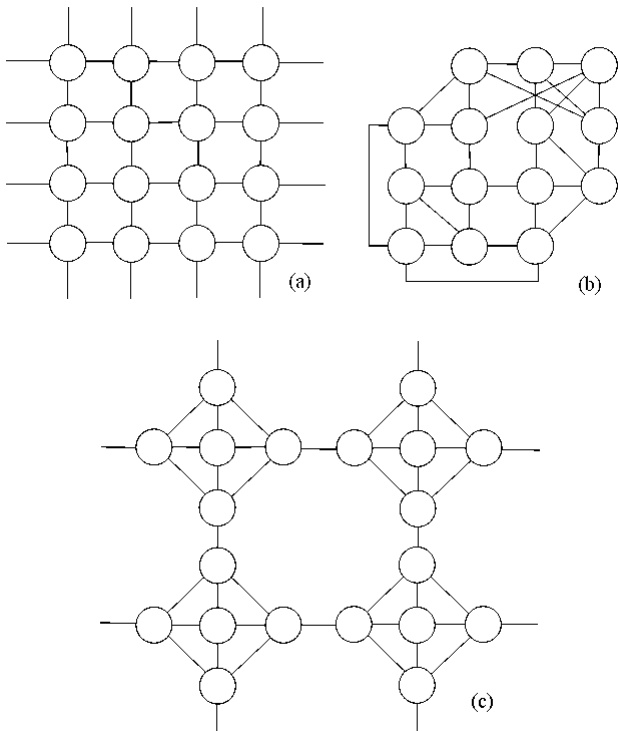


FIG. 1: Three examples of ‘regular’ graphs, with all nodes with degree equal to 4.

work is that every node would be undistinguishable from any other node. Therefore, identical measurements (e.g. node degree, clustering coefficient, hierarchical degrees, etc.) would be obtained for any of the nodes in the perfectly regular network. In this sense, regularity becomes closely related to symmetries in the networks.

However, as we want to achieve increased flexibility, in this work we relax the above definition and propose that a graph (or subgraph) is *regular* whenever all its nodes present similar values for a set of measurements. Therefore, this definition is relative to the allowed degree of values dispersion and the chosen set of measurements. Interestingly, the traditional regularity in graph theory can be understood as a particular instance of the above definition in the case of null dispersion (i.e. all degrees are identical) and selection of only the node degree as measurement. Here we consider non-null tolerance for the variability of the measurements (e.g. in order to cope with incompleteness or noise during the network construction) and a more comprehensive set of local measurements, defined for each node, including the degree, clustering coefficient, neighboring degree, and the locality index.

Two approaches are considered here in order to investigate the regularity of complex networks. We introduce these approaches with the help of Figure 2. The first involves the calculation of the dispersion of each specific

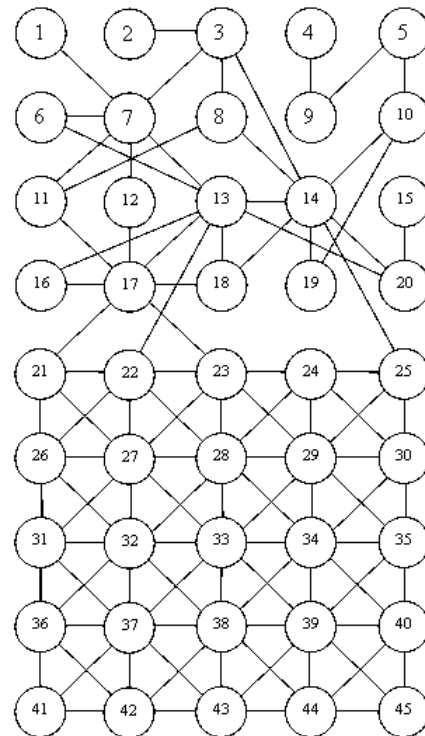


FIG. 2: An example of network including a regular subgraph (or patch).

measurements considering the successive neighborhoods (e.g. [8, 9, 10, 11, 12]) around each node. Although relatively simple and limited, this approach allows a preliminary indication about the possible participation of each node in a regular subgraph, as well as its level of ‘insertion’ inside such regular patches. Dispersions are calculated for each progressive neighborhood. For instance, the dispersion of the node degree for a given node i at the second neighborhood hierarchy (or level) is obtained by calculating the dispersion (e.g. standard deviation) of the set of nodes comprising the original node i , its immediate neighbors, and the neighbors of the latter. Therefore, a complete signature of dispersions is obtained for each node in terms of the several considered neighborhood hierarchies. Consequently, nodes which lie more internally the regular patches of the network will tend to present smaller dispersions along extended neighborhood hierarchies. For instance, in Figure 2, this kind of signature could be expected for node 33, which is the most internal node inside the regular patch of the network. Figure 3 presents the dispersion signatures (standard deviation) of node degree along 4 hierarchical levels (from 0, corresponding to the reference node, up to 3) obtained for nodes 17 (a) and 33 (b) in the graph of Figure 2. By convention, all signatures start with zero (i.e. only the original reference node, with no dispersion) and proceeds along the successive neighborhood levels. As expected, node 33 presents null dispersion of node degree

also for the subgraph obtained by considering that node and its immediate neighbors. Contrariwise, the signature obtained for node 17 presents relatively high values for hierarchical levels 1, 2 and 3.

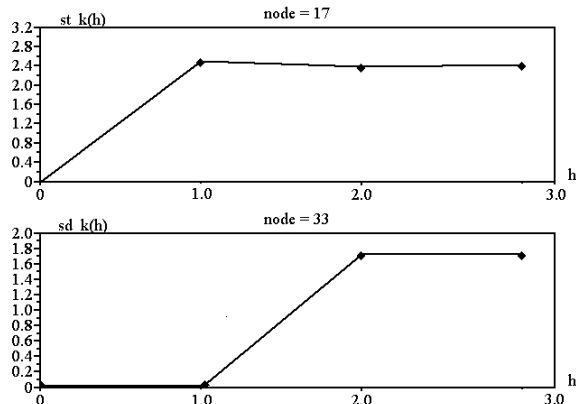


FIG. 3: The hierarchical standard deviations of nodes 17 (a) and 33 (b) from the graph in Figure 2 for the three first neighborhood hierarchies around those nodes. Observe that the node degree dispersions for node 33 stay with null value for the first two hierarchical neighborhood levels.

The limitation of the hierarchical approach outlined above stems from the fact that the progressive subgraphs are determined by successive dilations of the original node, irrespectively of the intrinsic similarity among the nodes in such expanding subgraphs. Consequently, the regular patches of the network can not be accurately determined by considering the hierarchical dispersions. An alternative way to approach the identification of regularity in complex networks is described as follows. This alternative methodology is aimed not at quantifying the regularity around each node (as the hierarchical dispersions method), but at obtaining the regular subgraphs present in the complex network under analysis. This is a more challenging objective. More specifically, several measurements are taken for each node in the network, and projected into a discrete two-dimensional phase-space (the accumulator array) by using principal component analysis (e.g. [7, 13, 14, 15]). Such a statistical mapping corresponds to a linear transformation (actually a rotation in the phase space) that ensures that the maximum dispersion of the points will be achieved along the first projection axes (i.e. those corresponding to the largest absolute values of eigenvalues of the covariance matrix of the data). The projection onto this two-dimensional phase space is performed by considering a given resolution for the two axes (binning), so as to obtain a two-dimensional *histogram*, here called accumulator array. Therefore, nodes which have similar measurements will appear close one another in the discrete two-dimensional phase space, contributing to a higher value of the histogram at that particular position. Consequently, every peak in such a histogram indicates the presence of several nodes with similar properties, which

may belong (or not) to regular patches in the network. However, because such nodes do not necessarily correspond to a connected component in the original network, we need to check the connectivity among them in order to identify eventual patches of regularity. Therefore, sets of nodes which are connected and have similar measurements (i.e. belong to the same peak) constitute a *regular patch* in the original complex network. For instance, in the case of the simple network in Figure 2, it would be expected that the nodes inside the regular region, and perhaps also the nodes at the border of this region, would constitute such a type of region. That is because those two sets of nodes have similar topological properties (e.g. node degree and clustering coefficient) and are connected among themselves.

The organization of the current work is as follows. After presenting a non-exhaustive summary of related works, the basic concepts (including the four considered network models and network local measurements) are briefly presented. Next, we introduce more formally the two suggested approaches for characterization of regularities inside complex networks and illustrate their potential with respect to theoretical models (i.e. Erdős-Rényi, Brarási-Albert, Watts-Strogatz and a simple geographical network) as well as to real-world complex networks (i.e. word associations, cortical nets, protein-protein interaction, football, and flights). Correlation and path analysis are also employed in order to obtain insights on how the topological measurements influence the regularity for each type of model. A series of interesting results are reported and discussed.

II. BRIEF REVIEW OF RELATED WORKS

To our best knowledge, no work has specifically addressed the issue of identifying regularities in complex networks. This issue is however related to at least the following four complex networks subjects: (i) assortativity; (ii) community finding; (iii) k-cores; and (iv) k-cliques. The problem of regularity in complex networks is revised with respect to these three areas in the following.

The concept of *assortative mixing*, developed by Newman [16] (see also [17]), quantifies the tendency of a node with high degree to connect with other nodes with high degree (the term *dissortative* has been used to express the opposite trend). Assortativity is related to regularity detection in the sense that maximum node correlation is observed for a regular network. At the same time, a network with high assortativity is not guaranteed to be strongly regular because the node degree is not sufficient to characterize this property (see Fig. 1 and respective discussion). Several networks have been found to exhibit specific patterns of assortativity or disassortativity. For instance, Newman and Park [18] showed that social networks tend to present assortative mixing between adjacent nodes, as opposite to most non-social

networks. That work also related assortativity and community structure in complex networks. The subject of assortativity and communities in social networks has also been investigated by Boguña et al. in [19]. The fact that scale-free networks tend to be disassortative has been addressed by Yook et al. [20]. The relationship between the node degree and the clustering coefficient has been studied by Serrano and Boguña [21], who showed that the level of assortativity establishes an upper limit to clustering. Related investigations have been addressed by Holme and Zhao [22].

Given a network, it is often possible to identify respective subgraphs whose nodes are more intensely connected one another than with the rest of the network. Such subgraphs are called the *communities* of the original network (e.g. [23, 24, 25, 26]). Such as communities, the regular patches sought in the current work are subgraphs of the original network which exhibit some peculiar property. However, while the nodes in a community share the overall property of being more intensely connected one another than with the remainder of the network, such a connectivity pattern can still be highly heterogeneous. In other words, communities are not necessarily regular patches and regular patches are not guaranteed to correspond to communities.

The concept of k -core has received increasing attention recently (e.g. [27, 28, 29, 30, 31, 32]). Given a network, its k -core can be obtained by repeatedly removing all nodes with degree smaller than k . Although the k -cores tend to be more degree regular, especially for larger values of k , they can still present substantial heterogeneities.

Finally, k -cliques are defined as fully connected subgraphs with k nodes (e.g. [33, 34, 35]). In particular a *k -clique percolation cluster* [34], which is similar to a regular percolation cluster, is a maximal k -clique connected graph, namely the union of all k -cliques which are connected. Though such k -clique clusters tend to exhibit regularity of node degree, the other measurements of their local connectivity (e.g. the clustering coefficient) can vary widely. A similar concept has been developed in terms of virtual links and conditional expansions [36]. More specifically, the connections of shortest path length 2 and 3 between nodes are identified and those nodes which are interconnected through such connections are suggested to form nearly regular subgraphs potentially associated to the network communities. Such a concept was also revisited more recently by Bagrow et al. [37]. The relationship between cliques and communities has been considered by Palla et al. [38].

The quantification of the symmetries at and around network nodes, which is also related to regularity characterization, has been studied by P. Holme [39]. The approach involves measuring the similarity between permutations of paths of a given length emanating from each node. This methodology has been illustrated with respect to protein-protein interaction.

III. BASIC CONCEPTS AND METHODOLOGY

The undirected network Γ under analysis is represented by its adjacency matrix K , such that $K(i, j) = K(j, i) = 1$ indicates the presence of an edge between nodes i and j , with $1 \leq i, j \leq N$. Self-connections (i.e. $K(i, i) = 1$) are not considered. Although the concepts and methods introduced in this article are immediately extensible to directed networks, here we restrict our attention on undirected networks.

Given such a network Γ , the *immediate neighborhood* of any of its nodes i is defined as the set of nodes which are connected to node i through a single edge (higher order neighborhoods, which involve neighbors of neighbors and so on, are defined below). The *degree* of each of any of its nodes i , henceforth abbreviated as $k(i)$, is defined as the number of edges attached to that node. The *clustering coefficient* of that node, represented as $cc(i)$, is calculated by dividing the number of edges between the immediate neighbors of i , i.e. $n(i)$, by the maximum possible number of connections between those nodes, i.e. $n_M = n(i)(n(i) - 1)/2$. A network such that all its nodes have exactly the same degree is said to be *regular*.

Two nodes i and j are said to be connected through a *path* in case it is possible to move from i to j . The minimal number of edges visited during such a movement is called the *shortest path length* between nodes i and j , which is henceforth abbreviated as $sp(i, j)$. Local measurements (or features) are henceforth understood to express properties of the connectivity at or near each node. Global measurements (or features) reflect the topological properties along substantial portions of the network. Therefore, the node degree and clustering coefficient are said to be *local*, while the shortest path length is a *global* measurement.

The h -th *hierarchical neighborhood* (or a *parallel* [12]) of a node i corresponds to the set of nodes which are connected to node i through shortest paths with length h (e.g. [12]). The union of the h -th hierarchical neighborhoods for $h = 0$ to H plus the interconnections between those nodes defines a subgraph of Γ which we call the *H -ball* of node i (see also the *rs-ring* [12]). The hierarchical dispersion of a measurement with respect to a node i corresponds to the calculation, in the original network, of that measurement considering the H -ball around i .

The *neighboring degree* (e.g. [17, 40, 41]) of a node i , henceforth expressed as $knn(i)$, corresponds to the average of the degrees of the immediate neighbors of i . The *locality index* (e.g. [40]) of a node i , henceforth abbreviated as $loc(i)$, corresponds to the ratio between the number of connections among the set of nodes comprising i and its immediate neighbors divided by the sum of the edges connected to all those nodes.

A. Theoretical Models

In this work we consider four theoretical models of network representing the main types of such structures, namely: Erdős-Rényi (random graph), Barabási-Albert (scale-free), Watts-Strogatz (small-world), as well as a simple geographical model (e.g. [42]). These models are briefly described in this section.

An Erdős-Rényi random graph – ER – is defined by a constant probability of connection between any pair of its nodes ([33, 43, 44]). In other words, it corresponds to a Poisson process along the connectivity, with rate γ . The Barabási-Albert model – BA – is characterized by preferential attachment (e.g. [3]). More specifically, starting with m_0 nodes, new nodes with m connections are progressively (one-at-a-time) attached to the growing network, so that the probability of connections is proportional to the degree of the existing nodes, giving rise to the ‘rich get richer’ paradigm. The Watts-Strogatz networks [3, 45] – WS – are small world and characterized by a special type of connectivity which is nearly regular. More specifically, it starts with the N nodes organized as a ring (or lattice) and each node is connected to its m adjacent neighbors in both directions. Then, a fraction α (in this work $\alpha = 1$) of edges are rewired in order to establish long range connections. Though simple, the geographical model – GG – considered in this work does incorporate the typical properties of a geographical network, i.e. each node has a well-defined position in an embedding space and the probability of connections is defined by the distance (Euclidean) between each pair of nodes. The GG networks considered in this work are constructed as follows (e.g. [42]). First, N nodes are distributed with uniform probability along an orthogonal lattice with $L \times L$ points, with $L > N$. Then, each node is connected to all other nodes which are at maximum Euclidean distance d from it.

All networks considered in this work have approximately the same number of nodes N and average degree $\langle k \rangle$. The latter condition is enforced with respect to the $m = \langle k \rangle / 2$ parameter of the BA model. More specifically, given m , the Poisson rate of the ER networks is determined as $\gamma = 2m / (N - 1)$. In the case of the GG model, we assume that $d = L \sqrt{2m / (N\pi)}$.

While the concepts and methodologies for regularity characterization and identification covered in this article are general to connected or disconnected networks, the following analysis and results assume that the network is connected, in the sense that any node can be reached from any other node through a path. In order to ensure connected networks, the largest connected component of each network generated by the four models above (the same scheme is adopted for the real-world networks) are detected and considered for subsequent analysis. Because of the relatively high connectivity considered in this work (well above the respective percolation critical densities), which imply mostly connected networks, such a filtering has minor effects.

B. Real-World Networks

This work considers seven real-world networks, including:

Word associations: This network was obtained as described in [46]. After an initial word (‘sun’) was presented by the computer, a human subject replied with the first word that came to his mind. The entered words are then presented in random order, but so as to ensure similar rates of presentation, by the computer, to which the subject reply as above. This network was found to present nearly scale-free node degree distribution.

Three Cortical Networks: Cortical networks are obtained from anatomical and functional experiments so that each node represent a cortical area and each edge a physical connection between two areas. Three such networks have been considered here: (i) cat without thalamus [47, 48]; (ii) cat with thalamus [47, 48]; and (iii) monkey [49].

Protein-Protein Interaction: This network, obtained from Barabási’s site [57] [50], describes the interactions between proteins of *S. cerevisiae* (yeast). More specifically, each node is a protein, and the edges indicate interaction (i.e. possible docking) between pairs of proteins. This network has been found to present the scale-free property.

Football: This network, obtained from Newman’s network data [58] [51], includes the American football games between Division IA colleges during regular season Fall 2000. This network provides an example of social interaction network.

US Flights: This network corresponds to the flights between most US airports in 1997 and was obtained from the Pajek database [52].

All these networks were symmetrized before the regularity analysis.

C. Standardization and Pearson Correlation Coefficient

Given a set of samples X_i , $i = 1, \dots, M$, of a random variable X , its average and standard deviation can be respectively estimated as

$$\langle X \rangle = \frac{1}{M} \sum_{j=1}^M X_j \quad (1)$$

$$\sigma_X = \left(\frac{1}{M-1} \sum_{j=1}^M (X_j - \langle X \rangle)^2 \right)^{0.5} \quad (2)$$

The *standardized* version of the random variable X is defined (e.g. [14, 15]) as

$$\tilde{X} = \frac{X - \langle X \rangle}{\sigma_X} \quad (3)$$

Observe that \tilde{X} has necessarily zero means and unit standard deviation. Also, most of its values are constrained inside the interval $[-2, 2]$.

Given two registered random variables [59] X and Y represented by a set of respectively sampled values, as well as their standardized versions \tilde{X} and \tilde{Y} , the Pearson correlation coefficient (e.g. [15, 53, 54]) between those two variables can be estimated as the correlation between \tilde{X} and \tilde{Y} , i.e.

$$P(X, Y) = \frac{1}{M-1} \sum_{j=1}^M (\tilde{X}_j)(\tilde{Y}_j) \quad (4)$$

It can be verified that $-1 \leq P(X, Y) \leq 1$. In case P is close to 1, the two random variables X and Y are said to be *positively correlated*, exhibiting a tendency to ‘vary together’. In case P is near -1, the two variables are understood as being *negatively correlated*, presenting a trend to ‘opposed joint variation’. In case P is near zero, the two random variables are said to be *uncorrelated*.

D. Path Analysis

Introduced by S. Wrigth [55] as a means to model statistical relationships between observed random variables, *path analysis* provides a series of interesting modeling features [53, 54]. In addition to allowing the comparison between alternative models, path analysis can be used in order to quantify the influences of several observed *independent* variables [60] on one or more dependent variables.

In the way it is considered in the current work, path analysis is practically equivalent to multilinear regression. In particular, we apply path analysis in order to quantify the influence of the several considered topological measurements of the network on the obtained regularity indices. Compared to the Pearson correlation analysis of the pairwise relationships between the topological measurements and regularity indicators, path analysis provide a less degenerate quantification of the relationships between these measurements. While the Pearson correlation considers projections of the overall data onto two axes, one corresponding to a topological measurement and the other to a regularity indicator, and then quantifies the linear relationship between those two variables, path analysis performs multilinear regression without any projection, i.e. considering the original multidimensional feature space. As a consequence, the influences of the independent over the dependent measurements becomes much more accurate and objective.

Figure 4 presents the path analysis model considered here. We have two dependent variables – namely the average of the number of peaks in the measurement histogram of the size of the maximum regular path detected in each network, which are assumed to depend on the 8 measurements of the networks topology – namely the

average and standard deviation of the node degree, clustering coefficient, neighboring degree and locality.

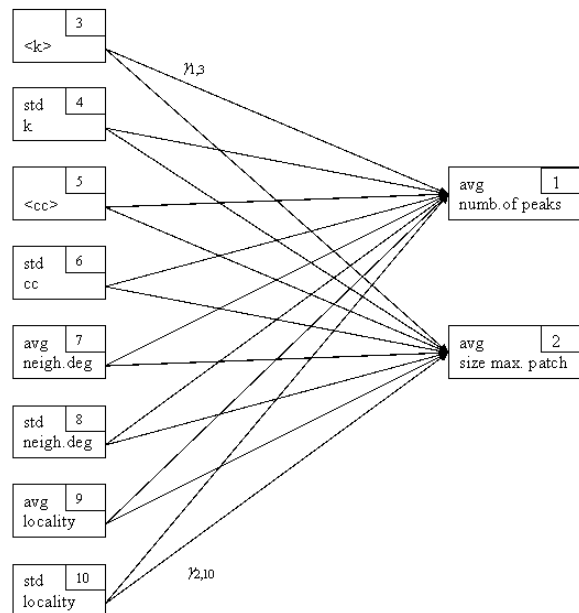


FIG. 4: The path analysis model considered in the present work. A total of 6 measurements of the networks topology are considered as independent variables which influence four dependent variables, namely the regularity indicators. The residues and respective covariances are not shown for simplicity’s sake.

The multilinear regression respective to the path analysis model in Figure 4 is given by the following equations:

$$P \propto \gamma_{1,5} \langle k \rangle + \gamma_{1,6} \sigma_{cc} + \gamma_{1,7} \langle cc \rangle + \gamma_{1,8} \sigma_{cc} + \gamma_{1,9} \langle knn \rangle + \gamma_{1,10} \sigma(knn) + \gamma_{1,11} \langle loc \rangle + \gamma_{1,12} \sigma(loc) \quad (5)$$

$$S \propto \gamma_{3,5} \langle k \rangle + \gamma_{3,6} \sigma_{cc} + \gamma_{3,7} \langle cc \rangle + \gamma_{3,8} \sigma_{cc} + \gamma_{3,9} \langle knn \rangle + \gamma_{3,10} \sigma(knn) + \gamma_{3,11} \langle loc \rangle + \gamma_{3,12} \sigma(loc) \quad (6)$$

Therefore, given the dispersions of the 8 topological measurements as well as of the two regularity indicators, path analysis will provide the influences $\gamma_{i,j}$ with respect to each pair of those features. In the present work, path analysis was performed in the LISREL environment [61].

E. Principal Component Analysis

Given M observations of a random vector \vec{v} composed of M random variables, these vectors can be represented in an M -dimensional phase space (or feature space) where each sample \vec{v}_i of \vec{v} defines a point. When M

is large, it is interesting to project the M -dimensional phase space into a space with smaller number W of dimensions. When W is 2 or 3, it becomes possible to visualize the phase space distribution. In addition, increased statistical representation is achieved in the lower dimensional space (the higher the number of dimensions, the larger the number of observations required to properly populate the phase space).

One possible way to project a distribution of points into a smaller dimensional phase space, with $W < M$ dimensions, is by using *principal component analysis* (e.g. [7, 13, 14, 15]). Such a statistical transformation involves three simple steps: (i) estimation of the covariance matrix of the original samples; (ii) calculation of the respective eigenvalues and eigenvectors; and (iii) use of the W eigenvectors associated to the largest absolute values of eigenvalues as the basis for projecting from the original to the dimensionally-reduced phase space.

IV. METHODOLOGY

This section presents the two main approaches considered in this work in order to study the regularity of complex networks, namely hierarchical measurement dispersions and the identification of connected regular patches.

A. Hierarchical Dispersions

Given a specific local measurement and a node i , its *hierarchical dispersion* is defined as the measurement of the dispersion inside the H -ball of i . Although several dispersion measurements – such as the standard deviation, coefficient of variation (i.e. the standard deviation divided by the average) and entropy – can be used, in this work we limit our attention to the former. The hierarchical dispersions are calculated with respect to the values of a chosen measurement along the several hierarchies around a given reference node.

Figure 5 presents the hierarchical standard deviations of the node degree and clustering coefficient for the hierarchies 1 (a), 2 (b) and 3 (c) for each of the nodes in the network in Figure 2. Observe the reduced dispersion obtained for the nodes more internal to the regular patch.

B. Detection of Regular Patches

Unlike the methodology described in the previous section, which is aimed at the characterization of regularity around successive neighborhoods of a node, the detection of regular patches is aimed at identifying the possible presence of near-regular subgraphs in the original network. A possible methodology for obtaining regular patches is described in the following.

First, the set of measurements defining the regularity is selected. Though such a set may include just the node degree (compatible with the traditional concept of regular graphs), because we want to impose more strict demands on regularity it is necessary to consider additional features describing the network connectivity around each node. In this work we consider two sets of measurements. The first includes the node degree and clustering coefficient; the second incorporates these two measurements plus the immediate neighboring degree and the locality index.

Having chosen the set of measurements, it is necessary to identify those nodes which are characterized by small dispersion of the measurements. In this work such a step is implemented with the help of an *accumulator array* acc [62]. Although higher dimensional accumulator arrays could be considered, in this work we limit our attention to two-dimensional arrays. Therefore, as implied by its name, the accumulator array is an array of $Q \times Q$ elements which will be used as a histogram in order to store the number of nodes whose measurements fall within the same respective interval (two-dimensional bin) and can therefore be understood as being regular. In case the set of measurements includes two features (e.g. node degree and clustering coefficient), the accumulator array indices are directly related to the measurements; otherwise principal component analysis (see Section III E) is used in order to project from the higher dimensional measurement space into two projected variables related to the accumulator array indices.

Let μ_1 and μ_2 be the two measurements to be mapped into the accumulator array, with minimum and maximum values given respectively as $min(\mu_1)$, $min(\mu_2)$ and $max(\mu_1)$, $max(\mu_2)$. Also, let the two indices of the accumulator array be represented as i and j , with $1 \leq i, j \leq Q$. The resolutions of these two measurements are given respectively as:

$$\Delta\mu_1 = \frac{max(\mu_1) - min(\mu_1)}{Q - 1} \quad (7)$$

$$\Delta\mu_2 = \frac{max(\mu_2) - min(\mu_2)}{Q - 1} \quad (8)$$

The original measurements can now be mapped into the accumulator array indices by using the following equations:

$$i = Round\left(\frac{\mu_1 - min(\mu_1)}{\Delta\mu_1}\right) \quad (9)$$

$$j = Round\left(\frac{\mu_2 - min(\mu_2)}{\Delta\mu_2}\right) \quad (10)$$

In the current work, the resolutions $\Delta\mu_1$ and $\Delta\mu_2$ are always set as corresponding to 1/10 of the excursion of the respective measurements μ_1 and μ_2 , i.e. $Q = 11$.

Now, given a network, the above mapping is performed for every node and the respective accumulator array cell

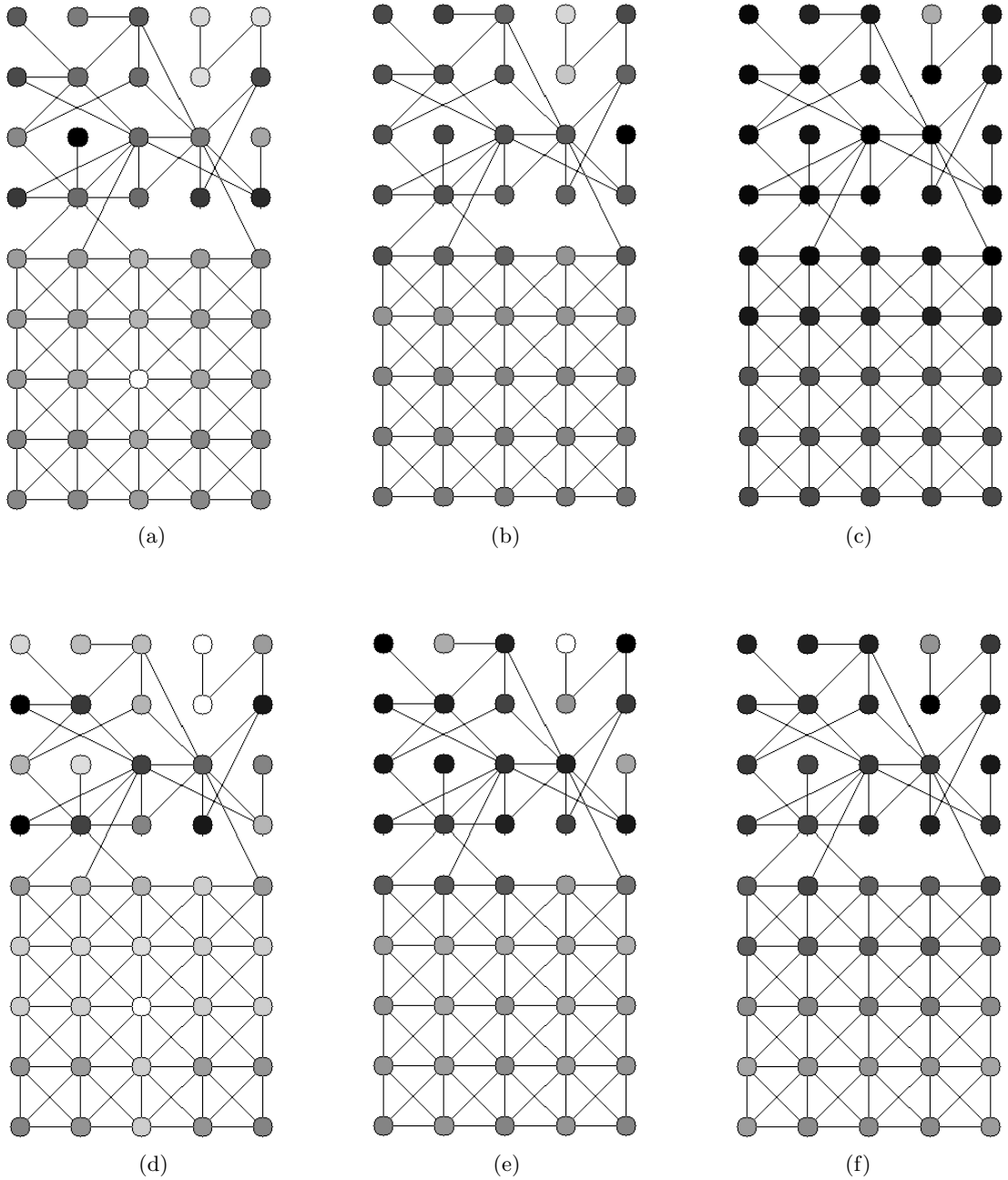


FIG. 5: The hierarchical standard deviations of the node degree obtained for the nodes of the simple network in Figure 2 with respect to hierarchy 1 (a), 2(b) and 3(c). The hierarchical standard deviations of the clustering coefficient obtained for that same graph for hierarchies 1 (d), 2 (e) and 3 (f). Observe that darker gray levels indicate higher dispersion values.

is incremented by one every time the measurements of a node fall at that cell. At the end of this procedure, peaks in the accumulator array will indicate set of nodes which have similar measurements. However, the nodes defining a peak do not necessarily correspond to a regular patch, as they may not be connected in the original graph. Therefore, the last step in the regular patch detection corresponds to obtaining the connected subgraphs for each considered peak in the accumulator array. Two

indicators of the regularity of the network under analysis are considered in the current work: (i) the number of detected peaks P ; and (ii) the size S of the maximum component identified for the maximum peak in the accumulator array. When comparing results obtained for networks with different sizes, it is interesting to consider also the value S/N . Henceforth, a cell of the accumulator array is considered as a peak whenever $acc(i, j) \geq N/10$, i.e. in case the accumulated count $acc(i, j)$ is larger or

equal than one tenth of the size of the original network. Observe that the size of the maximum component is obtained for the largest count (the maximum peak) in the accumulator array irrespectively of whether it exceeds or not the threshold $N/10$. It is also interesting to notice that the above methodology can be easily modified in order to try to detect additional regular patches defined by all peaks.

Figure 6(a) illustrates the accumulator array obtained for the network in Figure 2. The maximum peak, indicated as *A* in the figure, includes the nodes 24, 26, 30, 31, 35, 36, 40, 42, 43 and 44, which clearly correspond (see Figure 2) to the nodes belonging to the border of the near-regular region of network. Because all these nodes are connected, they constitute a single regular patch *R1* associated to the maximum detected peak. The second highest peak, indicated as *B* in Figure 6, is defined by nodes 27, 28, 29, 32, 33, 34, 37, 38, 39, which clearly correspond to the nodes inside the near-regular region of the network. Again, all such nodes are connected in the original graph, therefore defining a single detected regular patch *R2*. Observe that it is completely reasonable to obtain two regular patches, as the properties of the nodes in *R1* are clearly distinct to those of the nodes in *R2*. Figure 6(b) shows the accumulator array obtained by considering four measurements (i.e. node degree, clustering coefficient, immediate neighborhood degree and locality) projected through PCA. Now a sharp maximum is obtained, marked as *A* in the figure, which includes eight nodes: 21, 24, 26, 30, 36, 40, 42, 44, which again correspond to the border of the near-regular region of the original network. The fact that fewer pronounced peaks were obtained while considering more measurements is reasonable and reflects the stricter regularity conditions imposed by the additional measurements.

V. THEORETICAL MODELS

This section presents the results of hierarchical dispersion characterization and regular patch detection performed with respect to the four theoretical models of complex networks discussed in Section III A.

A. Hierarchical Dispersions

The hierarchical standard deviation of the node degree and clustering coefficient were obtained for the first three hierarchical levels for all nodes in the considered theoretical models of networks. All simulations in this section considered $N = 100$ and $m = 3$. Recall that the dispersion is calculated for a given hierarchical level h by considering all levels from 0 to h .

Figures 7– 10 show the dispersion (standard deviation) of the node degrees (lefthand-side column in each figure) and of the clustering coefficients (righthand-side column) for the ER, BA, WS and GG models, respec-

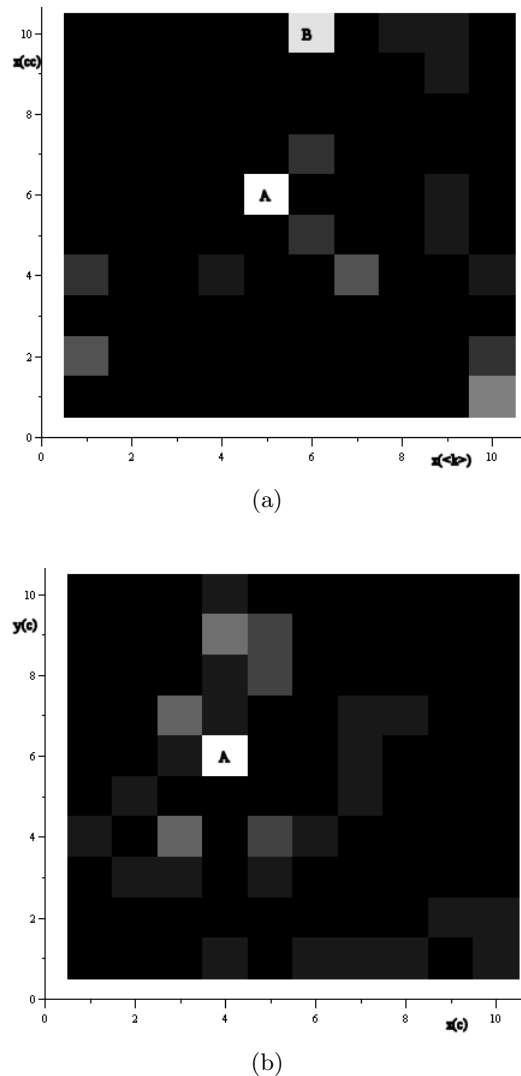


FIG. 6: The accumulator array (a) obtained for the network in Figure 2 considering the node degree and the clustering coefficient. The accumulator array obtained by using also the immediate neighborhood degree and the locality is presented in (b). Higher accumulated values are indicated by brighter levels.

tively. Little variation can be observed along the three hierarchical levels for the standard deviation of the node degree in the case of the ER networks (Fig. 7(a-c)), while the distribution of clustering coefficient standard deviations tended to be shifted to the right for the higher hierarchies (Fig. 7(d-f)). A completely distinct situation was obtained for the BA networks (Fig. 8), where the dispersions of the node degree and clustering coefficient changed substantially along the hierarchies. Of particular interest is the comparison between the distribution of node degree dispersions for the ER and BA models (Figs. 7 and 8). It is clear from Figure 8 that the BA networks have nodes with a wide range of degree regularities at the first hierarchical level, while the dispersion

of degrees is more stable for the ER models (Fig. 7). This can be understood as a direct consequence of the fact that the BA networks are characterized by intense diversity of node degrees, while the ER models can be well described by nearly regular node degrees. However, the diversity of degree dispersions decreases steadily for the higher hierarchical levels for the BA networks (Figs. 8(b-c)). Observe that the dispersion of the clustering coefficient in the BA model tends to increase with the hierarchies, i.e. it tends to become smaller for the first hierarchical level (Fig. 8d) than at the second (Fig. 8e) and third levels (Fig. 8f).

The dispersions of node degree observed for the WS networks (Figs. 9(a-c)) are very close to zero. In other words, the node degrees along successive levels change very little. This is expected because the WS model corresponds basically to a degree regular network with small irregularity caused by the few rewirings. The dispersion of the clustering coefficient are similar for the three hierarchical levels (Figs. 9(d-f)). In the case of the GG model, the degree dispersion was relatively small and changed little along the hierarchical levels (Figs. 10(a-c)). On the other hand, the distribution of clustering coefficient dispersions tend to be shifted to the right with the hierarchies (Figs. 10(d-f)).

Generally, by comparing the dispersion results obtained for all the four models, it becomes clear that the greatest degree regularity is observed for the WS model, which also presents relatively small values of clustering coefficient dispersions for all hierarchies. Small degree and clustering dispersions were also found for the ER model. Interestingly, the GG networks have small degree dispersions for all hierarchies, but present relatively high dispersions of clustering coefficient which tend to increase with the hierarchies. Finally, the BA networks exhibited the largest dispersions of degree and clustering coefficients, which tend to vary strongly with the hierarchical levels. These results are compatible with what could be expected regarding the intrinsic regularity of the ER, WS and GG models and the intense irregularity of the BA networks. However, the results obtained for the clustering coefficient dispersion in the case of GG model show that this type of network is surprisingly irregular as far as this measurement is concerned. Because of the uniform distribution of the nodes along the space in the considered GG model, the number of nodes at given distances from each node tends not to vary too much, which is not the case with the clustering coefficient.

B. Regular Patch Detection

Figure 11 shows, for each of the four considered models (500 realizations, with $N = 200$ and $k = 6$), the histograms of the number of peaks (i.e. the number of accumulator cells with count exceeding $0.1N$) and the size of the maximum connected component detected for each maximum peak obtained by regular patch detection

(see Section IV B) while taking into account the node degree and clustering coefficient.

Interestingly, similar results were obtained for the ER and BA models, with relatively broad distribution of numbers of peaks and of sizes of maximum components. Most such networks yielded from 2 to 4 peaks (a,c). At the same time, the maximum components detected for each peak had sizes ranging from 0 to about 50 nodes (b,d). The highly skewed histograms obtained for the latter measurement indicate that most frequently such maximum components (which are regular patches) had small size. Although a similar distribution of maximum component sizes was obtained for the GG model (h), the respective histogram of number of peaks resulted very peculiar, with most situations corresponding to zero detected peaks. The results obtained for the WS are substantially distinct from those obtained for the ER and BA models: a total of two detected peaks was obtained for the vast majority of realizations (c), while the size of the maximum components was substantially larger than those obtained for the ER, BA or GG models.

The results obtained for the same networks, but considering the immediate degree and the locality in addition to the previously used node degree and clustering coefficient, are presented in Figure 12.

The consideration of the additional measurements had interesting effects on both the number of peaks and the size of the maximum detected component. In most cases, no peak was detected for the ER model (a), while the respective distribution of sizes resulted with similar form but substantially smaller average than obtained while considering only the node degree and clustering coefficient. Similar reductions were obtained for all other cases, with the GG model resulting in a larger mean of sizes than the BA networks (i.e. the opposite of the situation obtained above). Such reductions of the maximum detected component sizes can be understood as a consequence of the fact that the consideration of the two additional measurements implied stricter demands on the regularity required for a subgraph to qualify as a regular patch.

C. Correlation Analysis

Tables I(a-d) present the Pearson correlation coefficients obtained for each of the simulated types of models. These results are respective to regular patch detection by considering the node degree and clustering coefficient only.

Interestingly, the number of peaks P showed little correlation with all measurements and network types, except for the BA model, where it was found to be negatively correlated (-0.33) with the size of the maximum detected component S . Such a negative correlation is reasonable in the sense that a larger number of peaks indicate more, and consequently smaller, connected components. The fact that such a correlation was meaningful only for the

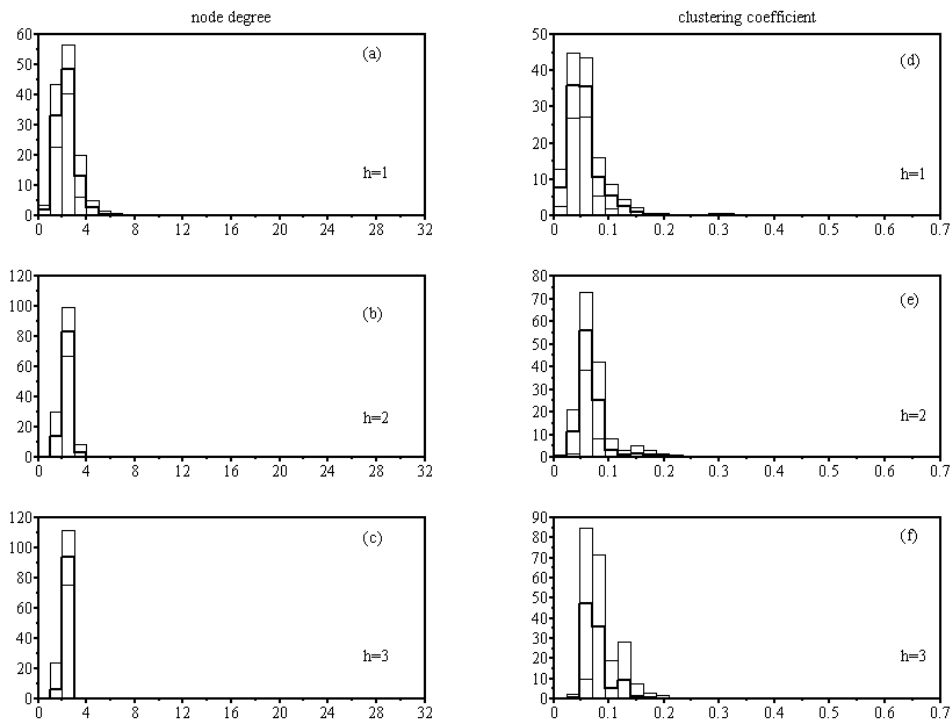


FIG. 7: The dispersion (standard deviation) of the node degrees (lefthand column) and of the clustering coefficients (righthand column) obtained for the three first hierarchical levels (three rows in the figure) for the ER model with $m = 3$ and $N = 100$. The thicker histogram shows the average values and the two thinner histograms the standard deviation.

BA model may be related to the fact that, among the four considered models, this is that less likely to produce regular patches.

The size of the maximum detected component S presented small correlations with all other measurements, except for the BA networks. In that case, the size S correlated negatively with the average node degree (-0.27) and positively with the dispersion of the average degree (0.42), the average and standard deviation of clustering coefficient (0.32 and 0.30, respectively), with the average and standard deviation of the immediate degree (0.41 and 0.51, respectively) and with the average locality (0.27). The negative correlation can be understood in the sense that, because of the intrinsic irregularity of the BA model, the more connected this type of network is, the less likely is the presence of regular patches. The largest positive correlations are more difficult to be explained, but should also reflect the rarity of regular patches in BA networks.

Other particularly intense correlations were observed between the average degree and average immediate degree in the case of the ER, WS and GG models (0.96, 0.94 and 0.99, respectively), between the average and standard deviation of the clustering coefficient (0.99) in the case of BA networks, and between the standard deviations of the node degree and immediate degree (0.97) for the GG model.

D. Path Analysis

The results of path analysis considering the model in Figure 4 and regular patch detection by using the node degree and clustering coefficient are given in Table II.

As expected, the influences of each of the eight topological measurements varied for the different types of networks. For the ER model, the number of peaks P was found to depend negatively on the average clustering coefficient (-2.06) and positively on the standard deviation of the clustering coefficient (5.09). This can be understood as a direct consequence of the fact that in a nearly regular network such as the ER model, a larger dispersion of clustering coefficient tends to break the regular patches. The size of the maximum detected component S was negatively affected by the average degree (-1.50) and positively by the standard deviation of the immediate degree (1.65). These two trends are somewhat counterintuitive (e.g. higher standard deviation of the immediate degree should promote regularity and therefore increase the size of the maximum component). In the case of the BA model, the most intense positive influence on P was from the average clustering coefficient (2.33), while the strongest negative influence originated from the average immediate degree. This positive influence possibly has the same explanation as for the similar effect observed for the ER case. On the other hand, S resulted strongly influenced by the standard deviation of

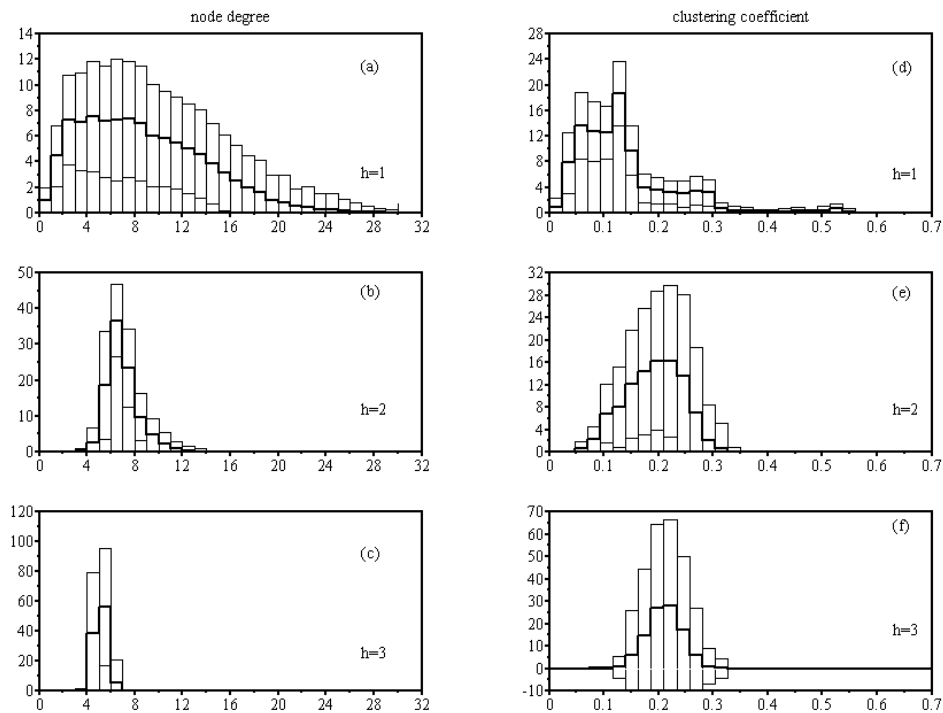


FIG. 8: The dispersion (standard deviation) of the node degrees (lefthand column) and of the clustering coefficients (righthand column) obtained for the three first hierarchical levels (three rows in the figure) for the BA model with $m = 3$ and $N = 100$. The thicker histogram shows the average values and the two thinner histograms the standard deviation.

the immediate degree (7.74) and negatively by the average immediate degree (-2.49). Such influences are again counterintuitive. Less intense influences were found for the WS model. In this case, P was particularly affected (negatively) by the standard deviation of the clustering coefficient (-1.68), while S was positively influenced by the standard deviation of the immediate degree (1.68). Both such effects are counterintuitive. In the case of the GG networks, P resulted strongly affected (negatively) by the standard deviation of the clustering coefficient (-3.21), and S was less affected by the considered topological measurements. Such a negative dependence between P and σ_{cc} was expected, as larger dispersions of the clustering coefficient tend to reduce the size of the maximum detected component.

As in [42], path analysis was particularly interesting for the identification of importance influences of the topological parameters over the regularity measurements, providing more objective results than could be obtained by correlation analysis. Of particular interest was the identification of particularly strong effects from the clustering coefficient and immediate neighborhood measurements, with relatively smaller influences from the locality and node degree. A number of trends, however, resulted counterintuitive and would require further investigations, possibly by using additional topological measurements.

VI. REAL-WORLD NETWORKS

The application of the regular patch extraction methodology to the real networks presented in Section III B is reported in this section. In addition to the number of peaks and size of maximum detected component, the number of nodes in the maximum peak (N_P) has also been considered. Table III presents the therefore obtained results for each of the real networks.

A series of interesting results can be identified. First, rather distinct numbers of peaks and sizes of maximum detected component were obtained for each of the networks. As quantified by the S/N index, the size of the maximum detected component varied from less than 1% (for the word associations, protein-protein interaction and flights networks) to about 10% (for the football and cortical networks). The three networks with the smallest S/N have a strong scale-free nature, which acts in order to reduce the regular patches in number and size. The football network resulted the most regular of the analyzed networks. This is a possible consequence of the social nature of this network (WS-like), which tends to promote regularity. The three cortical networks also resulted markedly regular. Observe that the above results are generally compatible with the experiments reported in this work with respect to the four theoretical models.

Some interesting effects can be also identified for specific networks. For instance, the inclusion of the thalamus

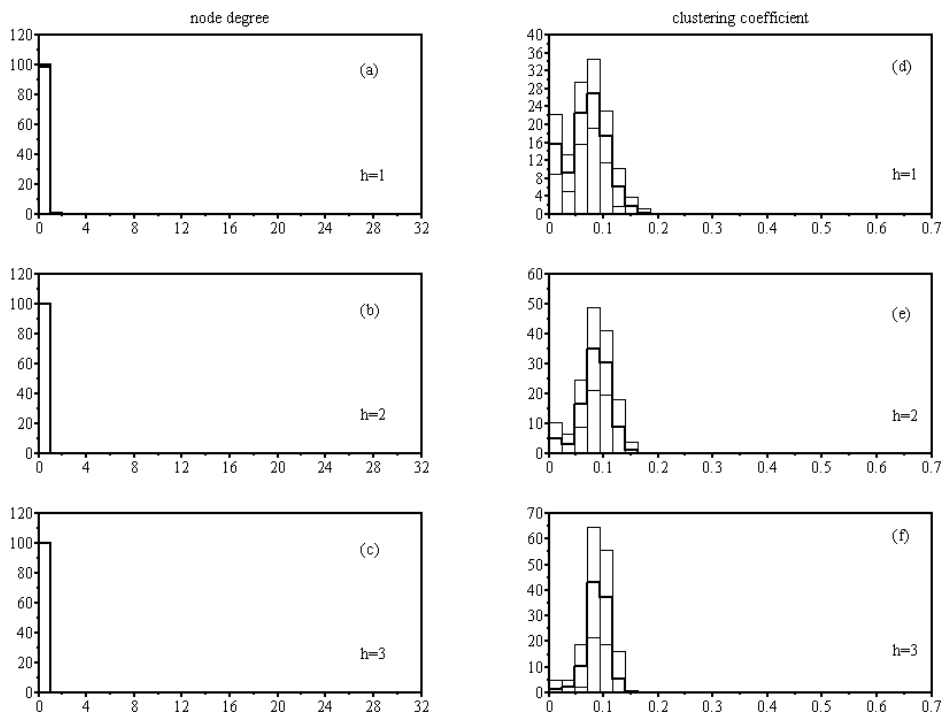


FIG. 9: The dispersion (standard deviation) of the node degrees (lefthand column) and of the clustering coefficients (righthand column) obtained for the three first hierarchical levels (three rows in the figure) for the WS models with $m = 3$ and $N = 100$. The thicker histogram shows the average values and the two thinner histograms the standard deviation.

in the cat cortical network tended to increase the regularity of the network, as suggested by the S/N measurements for the cat network without and with thalamus. The monkey network (without thalamus) resulted the highest S/N value among the cortical networks, which can be understood as a possible indication that more evolved brains would present a larger maximum regular patch. Particularly interesting is the fact that, despite its relatively large size ($N=1458$), the protein-protein interaction resulted few detected peaks and a rather small maximum detected component. Actually, out of the 1116 nodes (about 30% of the overall network) included in the maximum peak, the maximum connected component formed by these nodes included only 13 nodes. This result seems to indicate that the nodes not included in the maximum peak because of higher measurement dispersion are essential for the overall connectivity of that network. Therefore, each nearly regular node in the protein-protein interaction network tends to be connected with irregular nodes, defining a mosaic of regularity.

VII. CONCLUSIONS

Complex networks have achieved great importance as a consequence of their ability to represent and model real-world structures and systems, such as protein-protein interaction and the Internet and WWW, which involve in-

tricate and heterogeneous connectivity. Indeed, the older random networks (i.e. the ER model), characterized by intense regularity of node degree, have proved not to be particularly good for modeling natural phenomena. Therefore, a great deal of interest in complex network research has focused on the identification, analysis and modeling of *irregularities* (hence the name ‘complex’) in the connectivity of the networks. However, while such an irregularity, as with the concept of complexity, is particularly difficult to be defined, the consideration of the dual approach of characterizing the *regularity* of complex networks can provide interesting insights and results useful for network identification and analysis. Particularly interesting is the influence of regularities on dynamical processes unfolding on the networks, which is promising because most of the dynamical systems investigations and results are related to perfectly regular networks such as orthogonal and hexagonal lattices. To approach the problem of identifying regularities in complex networks has been the principal motivation of the current work.

One of the most important points related to the identification of simplicities in complex networks relates to the fact that in graph theory (and also complex networks), regularity has been mostly associated to uniformity of the degrees of the nodes in the network. Actually, in graph theory a regular network is defined as having all its nodes with the same degree. However, as motivated and illustrated in the current work, degree regularity is

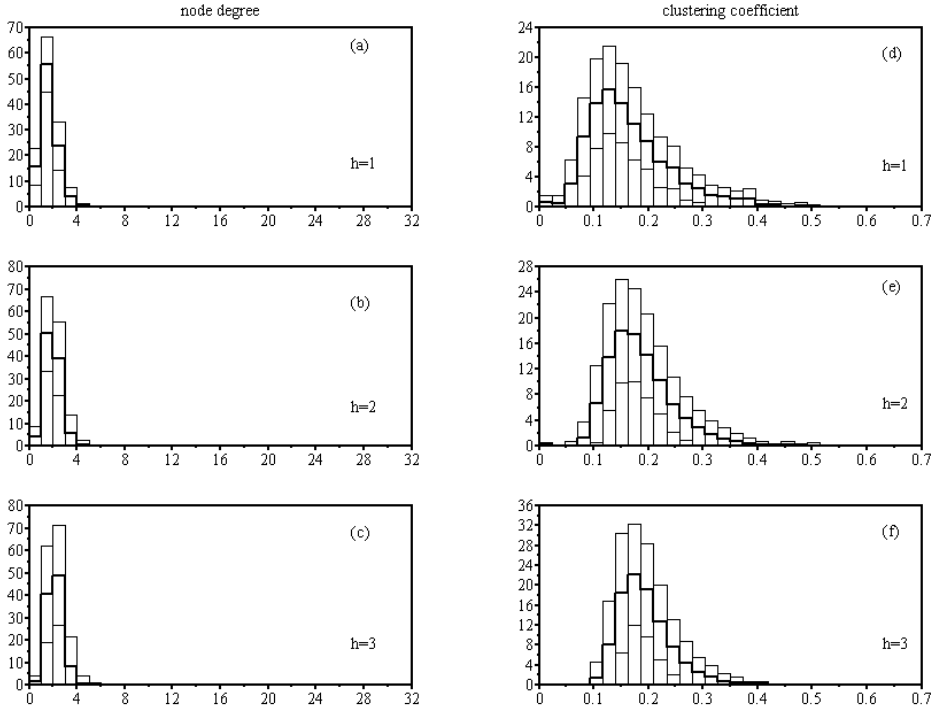


FIG. 10: The dispersion (standard deviation) of the node degrees (lefthand column) and of the clustering coefficients (righthand column) obtained for the three first hierarchical levels (three rows in the figure) for the GG models with $m = 3$ and $N = 100$. The thicker histogram shows the average values and the two thinner histograms the standard deviation.

far from being enough to characterize regularity (see, for instance, the examples in Figure 1). Here, we propose that regularity in complex networks is indeed associated to a larger number of measurements of the connectivity around each network node. Indeed, regularity is a concept associated to symmetry of the network, in the sense that in a perfectly symmetric network all possible topological measurements would result identical for every node. Because such a definition is too strict, we allow some degree of tolerance to measurements variation. More precisely, it is suggested that a regular patch of a network is a connected subgraph characterized by the fact that all its nodes have small dispersion of a set of chosen measurements. Two possible such sets have been considered in this work: (i) the node degree and clustering coefficient and (ii) these two measurements plus the neighboring degree and locality.

Having suggested a quantitative definition of what regularity means for complex networks, it was possible to devise two methodologies for its: one allowing the quantification of the regularity along successive hierarchical balls around each node, the other providing the means for identifying regular patches in networks.

The former methodology is based on the concept of hierarchical levels (or progressive neighborhoods) defined by taking each network node as a reference. For each subgraph defined by dilating the initial reference node up to the hierarchy h , the dispersion (in this work limited to

standard deviation) is calculated for each of the chosen measurements. Therefore, signatures of the dispersion evolution in terms of the hierarchical levels are obtained for each node and for each measurement. By considering the average and standard deviation of such signatures, it is possible to infer how the regularity of the network (or of a specific subnetwork) progress along successive neighborhoods. The potential of this approach for characterization of networks was illustrated in the current work with respect to four theoretical models, namely ER, BA, WS and GG. Several interesting results were obtained, including the fact that the WS tends to be the most regular network for the two considered sets of measurements. The ER and GG networks also exhibited a good deal of node regularity, but with varying dispersions of clustering coefficient. The BA networks proved to be the most irregular of all the four considered theoretical models with respect to all measurements.

The second methodology reported in this work was aimed at identifying regular patches in complex networks. This method involves four main steps: (i) estimation of measurements for each node; (ii) mapping of such measurements into a two-dimensional accumulator array (a two-dimensional histogram) by using principal component analysis; (iii) the identification of peaks in the accumulator array; and (iv) the verification of the presence of connected components in the original network, defined by the nodes in each peak. Every accumulator

array cell with count larger than 10% of the total number N of nodes in the network was considered a peak. The maximum peak corresponded to the cell with the highest count, even if its value did not exceed the above threshold. This method proved to allow the identification of extensive patches of regularity for some of the considered theoretical models of networks. The regularity of the networks was quantified in terms of the number of detected peaks as well as the size of the maximum detected component. The largest patches were detected for the WS model, followed by the ER, BA and GG. Interestingly, by considering node degree and clustering coefficient, the WS model always produced two detected peaks, while many networks were unable to produce peaks in the case of the GG model. By imposing stricter regularity conditions, the use of the additional measurements (neighboring degree and locality index) reduced the number of detected peaks and sizes of the maximum detected components.

In addition to the four theoretical network models, seven real-world networks were also considered in order to illustrate the application of the regularity patch detection. The considered networks included word associations, three cortical networks, protein-protein interaction, football league, and an airport network. As could be expected, those networks characterized by scale-free node degree (i.e. word associations, protein-protein interaction and flights) implied the smallest sizes of maximum detected components, while the football network (a kind of social network) and the three cortical networks resulted more regular. Specific insights were also obtained, including the effect of the thalamus in promoting a larger maximum regular path in the cat, and the interspersion of regular and irregular nodes in the protein-protein interaction network.

Correlation and path analyses were used in order to try to better understand the influence of the topological properties of the network on the regularity of the detected patches. While the correlation analysis resulted in weak relationships between the number of peaks and size of the maximum component and the topological measurements, path analysis again [42] proved to be an interesting means to quantify the influences of the topological features on the analyzed regularity properties. Two particularly important results were obtained through path analysis: (a) the influences of the topological measurements on the two regularity indices varied substantially among the four theoretical models of networks; and (b) topological parameters additional to node degree, especially the clustering coefficient and neighboring degree, proved to be particularly influent in defining the regularity properties.

All in all, we believe the reported methods and results illustrated and corroborated the importance of considering regularity in order to characterize and obtain insights about the properties of theoretical and real-world networks. Several are the possibilities for further investigations opened by this work, which include but are not

limited to the investigation of the effect of the average node degree, the consideration of other real-world networks, selection of additional topological measurements, the consideration of regular patches detected for secondary peaks (only the maximum patch defined by the highest peak was considered in this work), as well as the development of more precise methods for identifying the peaks in the accumulator array (e.g. a large regular patch may eventually become split between two or more adjacent peaks). With respect to the latter, extensive results from Hough transform studies (e.g. [56]) can be immediately applied. Last but not least, it is proposed that the regularity indices, possibly combined with other measurements, can provide an interesting means for identifying how much a given network is planar, in the sense of graph theory (i.e. the network can be drawn in a two-dimensional metric space without crossing edges).

List of Symbols

Γ = a graph or complex network;

N = number of nodes in a network;

K = the adjacency matrix of a complex network;

$k(i)$ = degree of a network node i ;

m = the parameter in the BA model defining its average node degree. This parameter is considered as reference for all network models in this work;

L = the size of the metric space where the geographical networks (GG) are defined;

$cc(i)$ = clustering coefficient of a network node i ;

$knn(i)$ = the neighboring degree of node i ;

$loc(i)$ = the locality index of node i ;

$\langle a \rangle$ = the arithmetic average of the property a ;

$\sigma(a)$ = the standard deviation of the random variable a ;

$\gamma_{i,j}$ = the influence (path analysis) of the measurement i over the measurement j ;

acc = the accumulator array obtained for a given network;

P = the number of peaks detected in the accumulator array for a given network;

S = the size of the maximum detected connected component;

N_P = the number of nodes in the maximum peak of the accumulator array;

Acknowledgments

Luciano da F. Costa thanks CNPq (308231/03-1) and FAPESP (05/00587-5) for sponsorship.

-
- [1] M. Gell-Mann, *The Quark and the Jaguar* (Owl Books, 1995).
- [2] K. Alligood, T. D. Sauer, and J. A. Yorke, *Chaos: An Introduction to Dynamical Systems* (Springer-Verlag, 1996).
- [3] R. Albert and A.-L. Barabási, *Reviews of Modern Physics* **74**, 48 (2002).
- [4] S. N. Dorogovtsev and J. F. F. Mendes, *Advances in Physics* **51**, 1079 (2002).
- [5] M. E. J. Newman, *SIAM Review* **45**, 167 (2003).
- [6] S. Boccaletti, V. Latora, Y. Moreno, M. Chaves, and D.-U. Hwang, *Physics Reports* **424**, 175 (2006).
- [7] L. da F. Costa, F. A. Rodrigues, G. Travieso, and P. R. V. Boas, *Characterization of complex networks: A survey of measurements* (2005), cond-mat/0505185.
- [8] M. Faloutsos, P. Faloutsos, and C. Faloutsos, *Computer Communication Review* **29**, 251 (1999).
- [9] M. E. Newman (2001), cond-mat/0111070.
- [10] R. Cohen, S. Havlin, S. Mokryn, D. Dolev, T. Kalisky, and Y. Shavitt (2003), cond-mat/0305582.
- [11] L. da F. Costa and F. N. Silva, *J. Stat. Phys.* (in press) (2007), URL cond-mat/0412761.
- [12] L. da F. Costa and L. H. C. da Silva, *Eur. Phys. J. B* **50**, 237 (2006), cond-mat/0408076.
- [13] R. O. Duda, P. E. Hart, and D. G. Stork, *Pattern Classification* (Wiley-Interscience, 2000).
- [14] L. da F. Costa and R. M. C. Jr., *Shape Analysis and Classification: Theory and Practice* (CRC Press, 2001).
- [15] R. A. Johnson and D. W. Wichern, *Applied Multivariate Statistical Analysis* (Prentice Hall, 2002).
- [16] M. E. J. Newman, *Phys. Rev. Lett.* **89**, 208701 (2002).
- [17] R. Pastor-Satorras, A. Vazquez, and A. Vespignani, *Phys. Rev. Lett.* **87**, 258701 (2001).
- [18] M. E. J. Newman and J. Park, *Phys. Rev. E* **68**, 036122 (2003), cond-mat/0305612.
- [19] M. Boguna, R. Pastor-Satorras, A. Diaz-Guilera, and A. Arenas (2003), cond-mat/0309263.
- [20] S.-H. Yook, F. Radicchi, and H. Meyer-Ortmanns (2005), cond-mat/0507198.
- [21] M. A. Serrano and M. Boguna (2005), cond-mat/0507535.
- [22] P. Holme and J. Zhao (2006), q.bio.OT/0611020.
- [23] F. Radicchi, C. Castellano, F. Cecconi, V. Loreto, and D. Parisi, *Proc. Natl. Acad. Sci. USA* **101**, 2658 (2004).
- [24] J. Reichardt and S. Bornholdt, *Phys. Rev. E* **74**, 016110 (2006), cond-mat/0603718.
- [25] M. E. J. Newman and M. Girvan, *Phys. Rev. E* **69**, 026113 (2004).
- [26] J. Reichardt and S. Bornholdt (2006), cond-mat/0606220.
- [27] S. B. Seidman, *Social Networks* **5**, 269 (1983).
- [28] J. I. Alvarez-Hamelin, L. Dall'Asta, A. Barrat, and A. Vespignani, *Adv. in Neur. Inform. Proc. Syst.* **18**, 41 (2006), cs.NI/0504107.
- [29] S. Carmi, S. Havlin, S. Kirkpatrick, Y. Shavitt, and E. Shir (2006), cond-mat/0601240.
- [30] S. Wuchty and E. Almaas, *BMC Evol. Biol.* **5**, 24 (2005).
- [31] S. N. Dorogovtsev, A. V. Goltsev, and J. F. F. Mendes, *Phys. Rev. Lett.* **96**, 040601 (2006), cond-mat/0509102.
- [32] A. V. Goltsev, S. N. Dorogovtsev, and J. F. F. Mendes, *Phys. Rev. E* **73**, 056101 (2006), cond-mat/0602611.
- [33] B. Bollobas, *Random Graphs* (Cambridge University Press, 2001).
- [34] I. Derenyi, G. Palla, and T. Vicsek, *Phys. Rev. Lett.* **94**, 160202 (2005), cond-mat/0504551.
- [35] G. Palla, I. Derenyi, and T. Vicsek (2006), cond-mat/0610298.
- [36] L. da F. Costa, *Phys. Rev. E* **70**, 056106 (2004), cond-mat/0312712.
- [37] J. Bagrow, E. Bollt, and L. da F. Costa (2006), cond-mat/0612502.
- [38] G. Palla, E. Derenyi, I. Farkas, and T. Vicsek, *Nature* **435**, 814 (2005), physics/0506133.
- [39] P. Holme (2006), cond-mat/0608695.
- [40] L. da F. Costa (2006), <http://arxiv.org/abs/physics/0607272>.
- [41] S. Maslov and K. Sneppen, *Science* **296**, 910 (2002).
- [42] L. da F. Costa (2007), URL physics/0701089.
- [43] P. Erdős and A. Rényi, *On random graphs* (1959).
- [44] P. Erdős and A. Rényi, *Bulletin of the International Statistical Institute* **38**, 343 (1960).
- [45] D. J. Watts and S. H. Strogatz, *Nature* **393**, 440 (1998).
- [46] L. da Fontoura Costa, *International Journal of Modern Physics C* **15**, 371 (2004).
- [47] J. W. Scannell, C. Blakemore, and M. P. Young, *The J. of Neurosc.* **15**, 1463 (1995).
- [48] J. W. Scannell, G. A. P. C. Burns, C. C. Hilgetag, M. A. O'Neil, and M. P. Young, *Cerebral Cortex* **9**, 277 (1999).
- [49] O. Sporns and J. Zwi, *Neuroinformatics* **2**, 145 (2004).
- [50] H. Jeong, S. Mason, A.-L. Barabasi, and Z. N. Oltvai, *Nature* **411**, 41 (2001).
- [51] M. Girvan and M. E. J. Newman, *Proceedings of the National Academy of Science USA* **99**, 7821 (2002).
- [52] V. Batagelj and A. Mrvar, *Pajek datasets*, University of Ljubljana, Slovenia, <http://vlado.fmf.uni-lj.si/pub/networks/data> (2006).
- [53] T. Raykov and G. A. Marcoulides, *A first course in structural equation modeling* (Lawrence Erlbaum Associates, Mahwah, New Jersey, 2000).
- [54] R. B. Kline, *Principles and Practice of Structural Equation Modeling* (Teh Guilford Press, New York, 2005), second edition.
- [55] S. Wright, *Proc. Natl. Acad. Sci. USA* **6**, 320 (1920).
- [56] J. Illingworth and J. Kittler, *Comput. Vis., Graph., and Im. Proc.* **44**, 87 (1988).
- [57] <http://www.nd.edu/networks/resources.htm>
- [58] <http://www-personal.umich.edu/mejn/netdata/>
- [59] I.e. the two variables correspond to a same observation, and therefore can be represented as a random vector $\vec{V} = [X_i, Y_i]$.
- [60] The term independent is often used in path analysis terminology in order to express the fact that such observed variables are assumed not to depend on other variables considered in the model. Contrariwise, *dependent* variables in path analysis receive statistical influence from the independent variables.
- [61] <http://www.ssicentral.com/lisrel/index.html>
- [62] The accumulator array used in the current work is not to be confounded with that applied in the Hough transform (e.g. [56]), a technique for recognition of geometrical objects (e.g. lines and circles). The difference is that

in that transform image elements (usually pixels) are mapped into curves in the accumulator array. However, techniques for peak analysis developed in the context of

Hough transform can be applied to improve the detection of the regular patches.

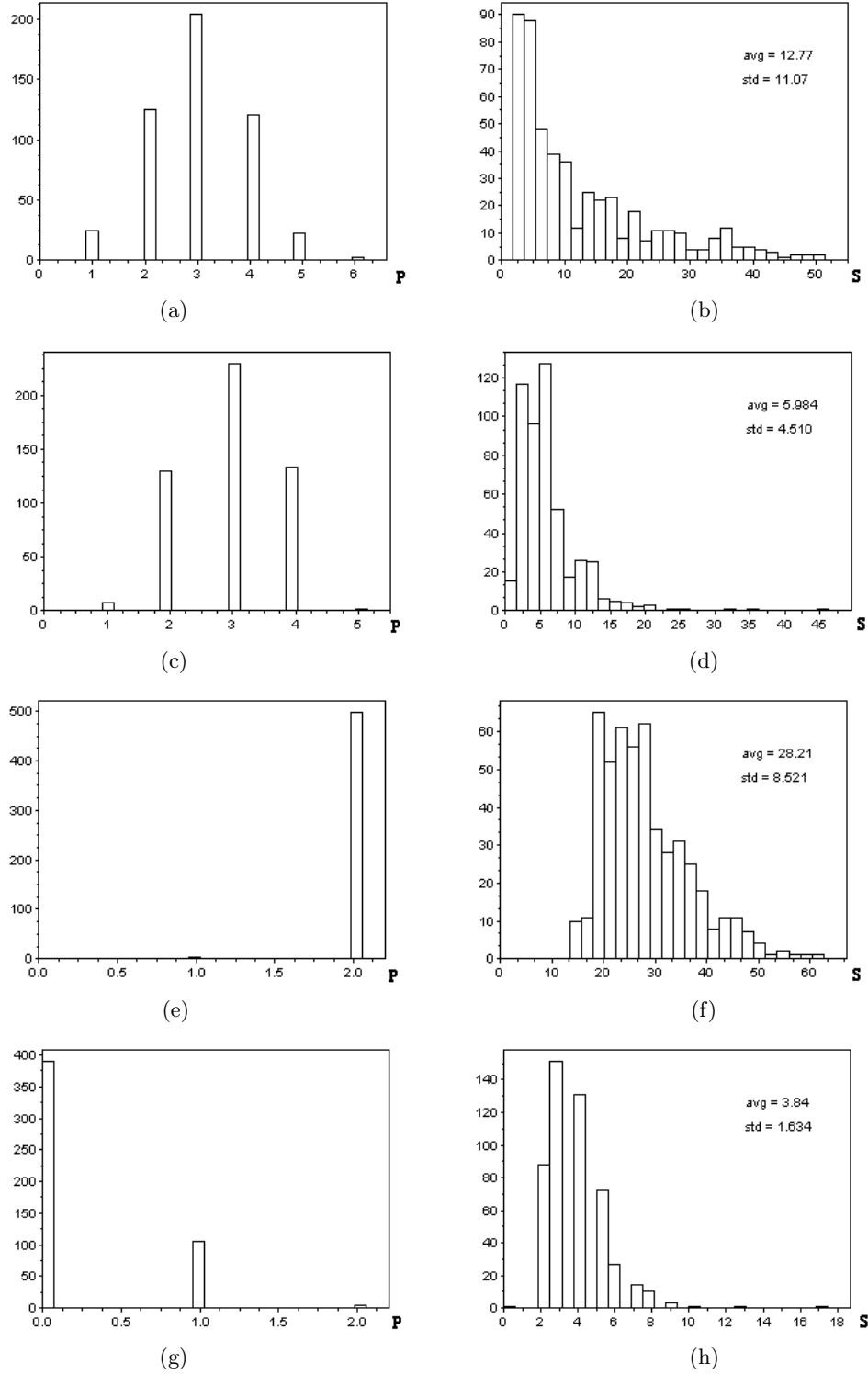


FIG. 11: The histograms of the number of detected peaks (P) and size of the maximum detected component (S) for each maximum peak obtained for 500 realizations of the ER (a-b), BA (c-d), WS (e-f) and GG (g-h) models with $N = 200$ and $m =$. The considered measurements were the node degree and clustering coefficient. The mean and standard deviation of the maximum component sizes are shown inside each respective histogram.

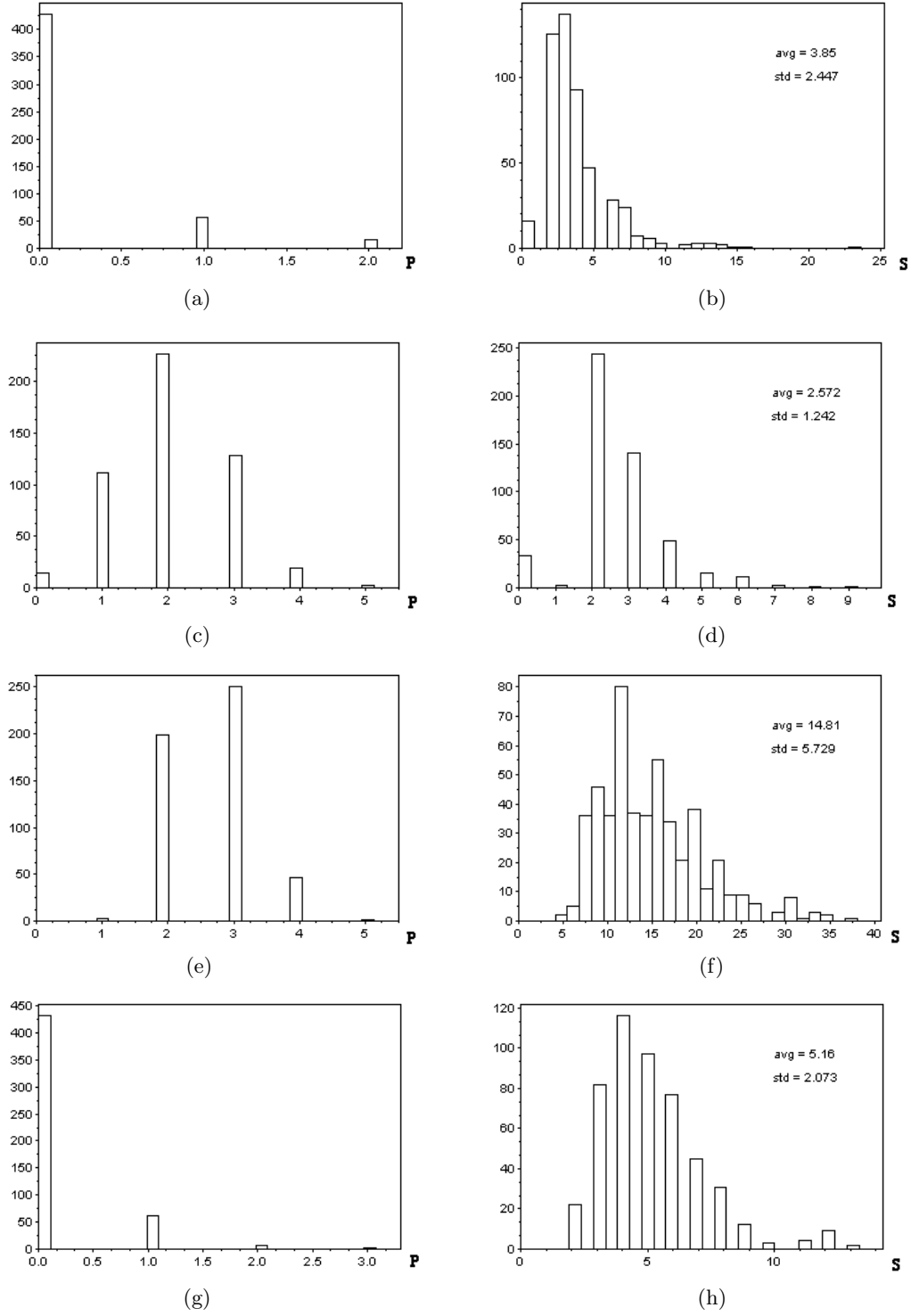


FIG. 12: The histograms of the number of detected peaks (P) and size of the maximum detected component (S) for each maximum peak obtained for 500 realizations of the ER (a-b), BA (c-d), WS (e-f) and GG (g-h) models with $N = 200$ and $m = 3$. The mean and standard deviation of the maximum component sizes are shown inside each respective histogram.

	P	S	$\langle k \rangle$	σ_k	$\langle cc \rangle$	σ_{cc}	$\langle knn \rangle$	σ_{knn}	$\langle loc \rangle$	σ_{loc}
P	1									
S	0.11	1								
$\langle k \rangle$	-0.20	-0.10	1							
σ_k	0.00	-0.11	0.42	1						
$\langle cc \rangle$	0.00	0.00	0.13	0.17	1					
σ_{cc}	0.26	-0.12	-0.18	0.04	0.71	1				
$\langle knn \rangle$	-0.17	0.00	0.96	0.62	0.16	-0.13	1			
σ_{knn}	0.04	0.03	0.00	0.66	0.01	-0.01	0.12	1		
$\langle int \rangle$	0.17	0.01	-0.41	-0.22	0.17	0.32	-0.86	0.18	1	
σ_{int}	0.10	0.00	-0.06	0.23	0.07	0.25	-0.33	0.61	0.57	1

(a)

	P	S	$\langle k \rangle$	σ_k	$\langle cc \rangle$	σ_{cc}	$\langle knn \rangle$	σ_{knn}	$\langle loc \rangle$	σ_{loc}
P	1									
S	-0.33	1								
$\langle k \rangle$	0.11	-0.27	1							
σ_k	-0.17	0.42	-0.42	1						
$\langle cc \rangle$	-0.02	0.32	-0.38	0.83	1					
σ_{cc}	0.00	0.30	-0.42	0.65	0.85	1				
$\langle knn \rangle$	-0.18	0.41	-0.42	0.99	0.83	0.65	1			
σ_{knn}	-0.03	0.51	-0.52	0.94	0.77	0.66	0.93	1		
$\langle int \rangle$	-0.04	0.27	-0.54	0.57	0.75	0.55	0.55	0.57	1	
σ_{int}	0.02	0.13	-0.22	0.22	0.35	0.30	0.22	0.23	0.76	1

(b)

	P	S	$\langle k \rangle$	σ_k	$\langle cc \rangle$	σ_{cc}	$\langle knn \rangle$	σ_{knn}	$\langle loc \rangle$	σ_{loc}
P	1									
S	-0.05	1								
$\langle k \rangle$	-0.02	0.06	1							
σ_k	-0.02	0.00	0.18	1						
$\langle cc \rangle$	-0.04	-0.01	-0.32	-0.04	1					
σ_{cc}	-0.09	0.16	0.26	0.17	-0.55	1				
$\langle knn \rangle$	-0.02	0.05	0.94	0.33	-0.30	0.29	1			
σ_{knn}	-0.06	0.06	-0.03	0.57	-0.11	0.15	0.08	1		
$\langle int \rangle$	-0.05	0.00	-0.38	-0.11	0.99	-0.56	-0.38	-0.11	1	
σ_{int}	-0.05	0.13	0.15	0.07	-0.70	0.88	0.15	0.11	0.67	1

(c)

	P	S	$\langle k \rangle$	σ_k	$\langle cc \rangle$	σ_{cc}	$\langle knn \rangle$	σ_{knn}	$\langle loc \rangle$	σ_{loc}
P	1									
S	0.27	1								
$\langle k \rangle$	-0.12	0.11	1							
σ_k	0.11	0.06	0.68	1						
$\langle cc \rangle$	-0.05	-0.10	0.32	0.13	1					
σ_{cc}	-0.11	-0.11	-0.55	-0.05	-0.28	1				
$\langle knn \rangle$	-0.12	0.11	0.99	0.70	0.32	-0.53	1			
σ_{knn}	-0.10	0.06	0.54	0.97	0.06	0.04	0.55	1		
$\langle int \rangle$	-0.08	-0.15	-0.21	-0.06	0.72	0.31	-0.21	0.00	1	
σ_{int}	-0.12	-0.07	-0.04	0.02	0.22	0.37	-0.03	0.02	0.37	1

(d)

TABLE I: Pearson correlation coefficients obtained for the ER (a), BA (b), WS (c) and GG (d) networks with $N = 100$ and $m = 3$ considering the number of peaks (P) and the size of the maximum detected component (S) and eight measurements of the topology of the network (i.e. average node degree ($\langle k \rangle$), standard deviation of the node degree (σ_k), average clustering coefficient ($\langle cc \rangle$), standard deviation of the clustering coefficient (σ_{cc}), average immediate degree ($\langle knn \rangle$),

standard deviation of the immediate degree (σ_{knn}), average locality ($\langle loc \rangle$) and standard deviation of locality (σ_{loc})).

		$\langle k \rangle$	σ_k	$\langle cc \rangle$	σ_{cc}	$\langle knn \rangle$	σ_{knn}	$\langle loc \rangle$	σ_{loc}
ER	P	$\gamma_{1,3} = -0.15$	$\gamma_{1,4} = 0.08$	$\gamma_{1,5} = -2.06$	$\gamma_{1,6} = 5.09$	$\gamma_{1,7} = 0.23$	$\gamma_{1,8} = 0.73$	$\gamma_{1,9} = 0.40$	$\gamma_{1,10} = -1.49$
	S	$\gamma_{2,3} = -1.50$	$\gamma_{2,4} = 0.27$	$\gamma_{2,5} = 1.02$	$\gamma_{2,6} = -0.09$	$\gamma_{2,7} = -0.62$	$\gamma_{2,8} = 1.65$	$\gamma_{2,9} = -2.10$	$\gamma_{2,10} = 0.83$
BA	P	$\gamma_{1,3} = 0.59$	$\gamma_{1,4} = -0.19$	$\gamma_{1,5} = 2.33$	$\gamma_{1,6} = 0.15$	$\gamma_{1,7} = -1.17$	$\gamma_{1,8} = -0.41$	$\gamma_{1,9} = -0.14$	$\gamma_{1,10} = -0.99$
	S	$\gamma_{2,3} = 0.47$	$\gamma_{2,4} = 1.17$	$\gamma_{2,5} = -0.57$	$\gamma_{2,6} = 0.31$	$\gamma_{2,7} = -2.49$	$\gamma_{2,8} = 7.74$	$\gamma_{2,9} = -0.16$	$\gamma_{2,10} = 0.70$
WS	P	$\gamma_{1,3} = -1.16$	$\gamma_{1,4} = -0.97$	$\gamma_{1,5} = 0.64$	$\gamma_{1,6} = -1.68$	$\gamma_{1,7} = 1.05$	$\gamma_{1,8} = 0.05$	$\gamma_{1,9} = -0.94$	$\gamma_{1,10} = 0.30$
	S	$\gamma_{2,3} = -0.69$	$\gamma_{2,4} = -1.07$	$\gamma_{2,5} = -0.73$	$\gamma_{2,6} = 1.63$	$\gamma_{2,7} = 0.89$	$\gamma_{2,8} = 1.68$	$\gamma_{2,9} = 1.07$	$\gamma_{2,10} = 0.32$
GG	P	$\gamma_{1,3} = -0.80$	$\gamma_{1,4} = -0.04$	$\gamma_{1,5} = 0.27$	$\gamma_{1,6} = -3.21$	$\gamma_{1,7} = 0.54$	$\gamma_{1,8} = 0.22$	$\gamma_{1,9} = -0.67$	$\gamma_{1,10} = -0.21$
	S	$\gamma_{2,3} = 0.82$	$\gamma_{2,4} = 0.10$	$\gamma_{2,5} = -0.85$	$\gamma_{2,6} = -0.65$	$\gamma_{2,7} = -0.70$	$\gamma_{2,8} = -0.06$	$\gamma_{2,9} = -0.20$	$\gamma_{2,10} = 0.04$

TABLE II: The influences of each considered topologic measurement on the two regularity measurements (P and S) as revealed by path analysis considering $N = 100$ and $m = 3$. These results are respective to regular patch detection by considering node degree and clustering coefficient.

Real Network	N	P	N_P	S	S/N
word associations	302	5	45	2	0.007
cat cortex	53	0	4	4	0.075
cat cortex + thalamus	95	0	8	8	0.084
monkey cortex	32	0	3	3	0.094
protein-protein	1458	1	1116	13	0.009
football	115	2	25	18	0.157
flights (97)	332	2	81	3	0.009

TABLE III: The regularity measurements obtained for the seven considered real networks.

